Non-equilibrium effects on SF6 arc plasmas in decaying phases

doi: 10.1109/ICEPE-ST.2015.7368379

Non-Equilibrium Effects on SF_6 Arc Plasmas in Decaying Phases

Yasunori Tanaka
Faculty of Electrical Eng.,
Kanazawa University
Kakuma, Kanazawa 920-1192 Japan
tanaka@ec.t.kanazawa-u.ac.jp

Katsumi Suzuki
Dept. of Electrical. Eng.,
Tokyo Denki University
Senjuasahi, Adachiku, Tokyo 120-8551 Japan

***Abstract*— In this paper, the two-temperature chemically non-equilibrium model developed was used to study the effect of transient recovery voltage (TRV) application to residual SF_6 arcs. The residual SF_6 arcs were created under free recovery condition. The TRV with a rate of rise of recovery voltage of 0.1 kV/μs and 0.2 kV/μs were numerically applied to the residual arcs. As a result, the application of 0.2 kV/μs TRV causes the arc re-ignition with increasing electron temperature and the electron density near the upstream electrode. It was also found that the temperature evolution by one-temperature model is simulated almost only to the evolution in the heavy particle temperature.**

I. Introduction

A high-voltage gas circuit breaker extinguishes the arc plasma formed between the electrodes by strong SF_6 gas flow during a high current interruption. The SF_6 is widely used for arc quenching medium because it has extremely high arc quenching ability with chemically stable and non-toxic properties. Downsizing of such a gas circuit breaker is one issue to enhance its reliability, and to reduce the use of SF_6 amount, because SF_6 has a much higher global warming potential of 22800 than CO_2. To downside the circuit breaker, it is of great important to understand in detail arc quenching phenomena around current zero in SF_6 gas. One powerful tool for this purpose is numerical modeling of decaying SF_6 arcs. The conventional numerical models often uses local thermodynamic equilibrium (LTE) assumption for arcs in some processings. Under the LTE assumption, all reactions should have infinite reaction rates, and the all temperature should be the identical. However, the LTE assumption is not always valid because it takes finite time for some reactions to reach their chemical equilibrium (CE) conditions. Thus, the chemically non-equilibrium (Non-CE) model has been developed for SF_6 thermal plasmas in [1] − [11].

In a circuit breaker, the decaying arc plasma between the electrodes is also exposed by transient recovery voltage (TRV) after current zero. The TRV application may raise the electron temperature T_e higher than heavy particle temperature T_h. To consider this effect, modeling of two-temperature SF_6 arcs has been developed [4]−[8], [12]. However, there are only few researches to study the non-equilibrium effects taking accounts of reaction heat, thermodynamic and transport properties.

In this paper, the developed two-temperature chemically non-equilibrium (2T-NonCE) model has been used to study phenomena in decaying SF_6 arcs with TRV application. The TRV was applied with a rise of rate of recovery voltage (RRRV) of 0.1 kV/μs and 0.2 kV/μs. The TRV application with a RRRV of 0.1 kV/μs results in successful interruption, while that of 0.2 kV/μs shows interruption failure thermally in 10 μs after TRV application. For arc re-ignition cases, the tempo-spatial distribution of T_e and T_h by the 2T-NonCE model were indicated. We furthermore compared the T_e and T_h to the temperature by one-temperature chemically non-equilibrium (1T-NonCE) model. Finally, the electron density evolution in case of arc-reignition is shown in this paper.

II. Assumptions in a SF_6 arc model

The developed model assumes the following things in the SF_6 arc plasma for simplicity: (i) Axisymmetric structure, (ii) Laminar flow, (iii) Optically thin, (iv) Electron emission phenomena were not considered. (v) Evaporation of the electrode and the nozzle was neglected. (vi) 19 species SF_6, SF_5, SF_4, SF_3, SF_2, SF, S_2, F_2, S, F, SF^+, S_2^+, F_2^+, SF^-, S^+, F^+, S^-, F^-, e^- were taken into account as constituents in SF_6 arc plasmas. (vii) The electron temperature T_e is not always the same to the heavy-particle temperature T_h. (viii) Electrons, ions, and neutral particles have the same flow velocity.

A. Governing equations for SF_6 arcs

On the basis of the assumptions in the preceding section, the behavior of SF_6 arc plasmas is governed by the following equations:
Mass:

$$\frac{D\rho}{Dt} = -\rho(\nabla \cdot \boldsymbol{u}), \tag{1}$$

Momentum:

$$\rho\frac{D\boldsymbol{u}}{Dt} = -\nabla p + \nabla \cdot \boldsymbol{\tau}, \tag{2}$$

$$\boldsymbol{\tau} = \tau_{ij} = 2\eta\left[e_{ij} - \frac{1}{3}\delta_{ij}(\nabla \cdot \boldsymbol{u})\right] \tag{3}$$

Energy for heavy particles:

$$\rho_\mathrm{h} C_{\mathrm{v\,h}}\frac{DT_\mathrm{h}}{Dt} = -p_\mathrm{h}(\nabla \cdot \boldsymbol{u}) + \nabla \cdot \left(\lambda_\mathrm{tr}^\mathrm{h}\nabla T_\mathrm{h}\right) + Q_{\mathrm{e-h}} + Q_\mathrm{heat}^\mathrm{h} \tag{4}$$

$$Q^{\rm h}_{\rm heat} = \sum_{j=1(j\neq {\rm e})}^{N} \nabla\cdot(\rho D_j h_j \nabla Y_j) + \sum_{\ell=1(\beta^{\rm f}_{{\rm e}\ell}\cdot\beta^{\rm r}_{{\rm e}\ell}=0)}^{L} \Delta Q_\ell \quad (5)$$

Energy for electrons:

$$\frac{3}{2}kn_{\rm e}\frac{DT_{\rm e}}{Dt} = \nabla\cdot(\lambda^{\rm e}_{\rm tr}\nabla T_{\rm e}) - Q_{\rm e-h} + Q^{\rm e}_{\rm heat} \quad (6)$$

$$Q^{\rm e}_{\rm heat} = \nabla\cdot(\frac{1}{m_{\rm e}}\frac{5}{2}kT_{\rm e}\mathbf{\Gamma}_{\rm e}) + \sum_{\ell=1(\beta^{\rm f}_{{\rm e}\ell}\cdot\beta^{\rm r}_{{\rm e}\ell}\neq 0)}^{L} \Delta Q_\ell + \sigma_{\rm e}|E|^2 - P_{\rm rad} - Q^{\rm e}_{\rm exc} \quad (7)$$

Mass of species j:

$$\rho\frac{DY_j}{Dt} = \nabla\cdot(\rho D_j\nabla Y_j) + S_j, \quad (8)$$

$$S_j = m_j\sum_{\ell}^{L}(\beta^{\rm r}_{j\ell}-\beta^{\rm f}_{j\ell})\left(k^{\rm f}_\ell\prod_{i=1}^{N}n_i^{\beta^{\rm f}_{i\ell}} - k^{\rm r}_\ell\prod_{i=1}^{N}n_i^{\beta^{\rm r}_{i\ell}}\right) \quad (9)$$

The equation of state:

$$p = p_{\rm e} + p_{\rm h} \quad (10)$$

$$p_{\rm e} = n_{\rm e}kT_{\rm e} \quad (11)$$

$$p_{\rm h} = \sum_{j(j\neq {\rm e})}^{N} n_j kT_{\rm h} \quad (12)$$

Mass density:

$$\rho = \frac{p}{kT_{\rm e}\frac{Y_{\rm e}}{m_{\rm e}} + kT_{\rm h}\sum_{j=1(j\neq {\rm e})}^{N}\frac{Y_j}{m_j}} \quad (13)$$

Energy conversion by excitation:

$$Q^{\rm e}_{\rm exc} = \sum_{j=1(j\neq {\rm e})}^{N}\left[k(T^j_{\rm ex})^2\frac{\partial \ln Z_j(T^j_{\rm ex})}{\partial T^j_{\rm ex}} - kT_{\rm h}^2\frac{\partial \ln Z_j(T_{\rm h})}{\partial T_{\rm h}}\right]\nu_{\rm eh}n_{\rm e} \quad (14)$$

Energy conversion by elastic collision:

$$Q_{\rm e-h} = \sum_{j=1(j\neq {\rm e})}^{N}\frac{3}{2}k(T_{\rm e}-T_{\rm h})\frac{2m_jm_{\rm e}}{(m_j+m_{\rm e})^2}\nu_{\rm eh}n_{\rm e} \quad (15)$$

Effective reaction heat:

$$\Delta Q_\ell = E_{{\rm reac}\ell}\left(k^{\rm f}_\ell\prod_{i=1}^{N}n_i^{\beta^{\rm f}_{i\ell}} - k^{\rm r}_\ell\prod_{i=1}^{N}n_i^{\beta^{\rm r}_{i\ell}}\right) \quad (16)$$

where ρ: mass density, t: time, $\boldsymbol{u}$: gas flow vector, p: pressure, $\boldsymbol{\tau}$: stress tensor, η: viscosity, e_{ij}: unit tensor, δ_{ij}: Kronecker delta, T: temperature, $C_{\rm vh}$: effective specific heat at constant volume for heavy particles, $\lambda_{\rm tr}$: translational thermal conductivity, D_j: effective diffusion coefficient, h_j: enthalpy of species j, Y_j: mass fraction of species j, $P_{\rm rad}$: radiation power, ΔQ_ℓ: heating power from reaction heat of reaction ℓ, m_j: mass of species j, $\beta_{j\ell}$: stoichiometric coefficient of species j for reaction ℓ, $k^{\rm f,r}_\ell$: reaction rate coefficient for reaction ℓ, n_j: density of species j, $\nu_{\rm eh}$: collision frequency between the electron and heavy particles, $E_{{\rm reac}\ell}$: Reaction heat for reaction ℓ, k: Boltzmann constant, $\frac{D}{Dt} = \frac{\partial}{\partial t} + \boldsymbol{u}\cdot\nabla$ is the Lagrangian derivative.

By solving (8), we can obtain mass fraction for each of species in the SF_6 arc in chemically non-equilibrium condition. On the other hand, the energy equations for electrons and heavy particles were solved to derive the $T_{\rm e}$ and $T_{\rm h}$ with thermally non-equilibrium effects. Eq.(15) is the energy conversion between the electron and heavy particles to couple both energy conservations (4) and (6). Eq.(6) takes into account the equivalent energy conversion by excitation reaction through electron impact processes. In this expression we used the effective excitation temperature $T^j_{\rm ex}$ for species j [13]. The $T^j_{\rm ex}$ was also used for calculation of h_j and $C_{\rm Vh}$ for considering the effect of electronic excitation of species j.

B. Thermodynamic and transport properties, rate coefficients for reactions

The fluid calculation needs the thermodynamic and transport properties such as specific heat $C_{\rm vh}$, enthalpy h_j, translational thermal conductivity for heavy particles $\lambda^{\rm h}_{\rm tr}$, translational thermal conductivity for electrons $\lambda^{\rm e}_{\rm tr}$, viscosity η, and emission coefficient $P_{\rm rad}$. These properties were self-consistently calculated using the computed particle composition, both $T_{\rm e}$ and $T_{\rm h}$, and the collision integrals at each position at each calculation step. The transport properties were calculated on the first order approximation of Chapman-Enskog method.

The developed model accounts for 61 reactions such as the electron impact ionization, the electron attachment, the electron impact dissociation, other chemical reactions, and their backward reactions [9]. Temperature dependent rate coefficients for these reactions were used in literatures [4]−[8]. Rate coefficients for their backward reactions were calculated through the principle of detailed balance. Reaction rate coefficient was assumed to depend on $T_{\rm e}$ when the electron is included as reactants, otherwise it depends on $T_{\rm h}$.

C. Calculation space and boundary condition

The calculation space for the arc device is shown in Fig. 1. Between the electrodes, the arc plasma is established. The arc plasma is blown by SF_6 gas flow from the left hand side in Fig. 1. This calculation space is the r-z two-dimensional axis-symmetrical space. This space was divided by 153×170 mesh. In this calculation, the following boundary conditions were set: The nozzle and the electrode has a non-slip wall with u=v=0. At the axis, v and the radial derivatives of physical parameters of u, $T_{\rm e}$, $T_{\rm h}$, p and ρ were set to zero. At the inlet around z=0 mm, the gas flow and the temperature were set 10 m/s and 300 K, respectively. At the outlet, the axial derivatives of the parameters were set to zero. The pressure at one point of the outlet was fixed at 0.5 MPa. This calculation neglected thermal decomposition of the nozzle and evaporation of the electrode for simplicity.

The current and voltage applied to the arcs are presented in Fig. 2. First of all, the arc plasma was simulated

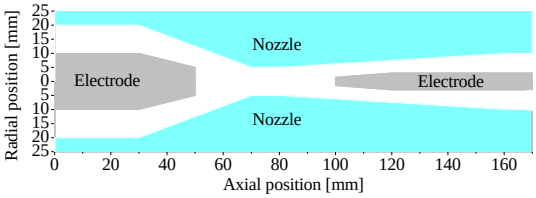

Fig. 1. Calculation domain.

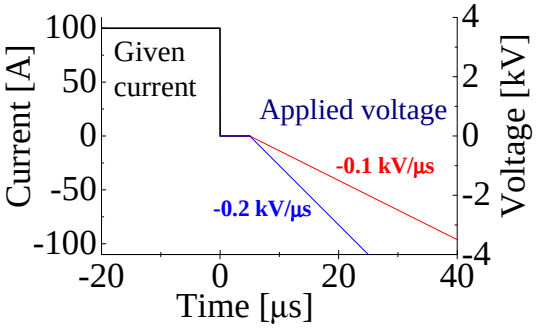

Fig. 2. Current and applied voltage given in the calculation.

under steady condition with a current of dc 100 A. From the steady state calculation, the decaying arc was simulated by stepping the current down from 100 A to 0 A. From t=5 μs after current down from 100 A to 0 A, TRV was applied with different RRRVs. The reason why a 5 μs delay was set before TRV application is that TRV application without a delay causes the large current, and then failure of current interruption. The values of RRRV in this paper are 0.1 kV/μs and 0.2 kV/μs. For transient calculation, the C-CUP algorithm was adopted.

III. Calculation Results

A. Tempo-spatial distribution of electron temperature and heavy particle temperature

The TRV application with a RRRV higher than 0.2 kV/μs causes interruption failure with involving continuously increasing post-arc current. On the other hand, the TRV application with RRRV$\leq$0.1 kV/μs resulted in the successful interruption with continuously decreasing post-arc current. It would be useful to study the aspect of arc re-ignition between the electrodes by TRV application with high RRRV. Figs. 3–6 illustrates the tempo-spatial distribution of temperature between the electrodes in an SF_6 arc at t = 0, 5, 7, and 8 μs after current zero. The upper panel in these figures shows the temperature T derived by a one-temperature chemically non-equilibrium (1T-NonCE) model previously developed [9] for comparison. The middle and lowest panels depicts respectively T_h and T_e obtained by the two-temperature chemically non-equilibrium (2T-NonCE) model in the present paper. Note that the TRV was initiated to be applied from t = 5 μs after current zero. The results at t = 0 μs in Fig. 3 are the same to those under steady state calculation for 100 A.

From current down at t=0 μs to t = 5 μs, both T_h and T_e decreases with time. Especially, T_e is rapidly diffused

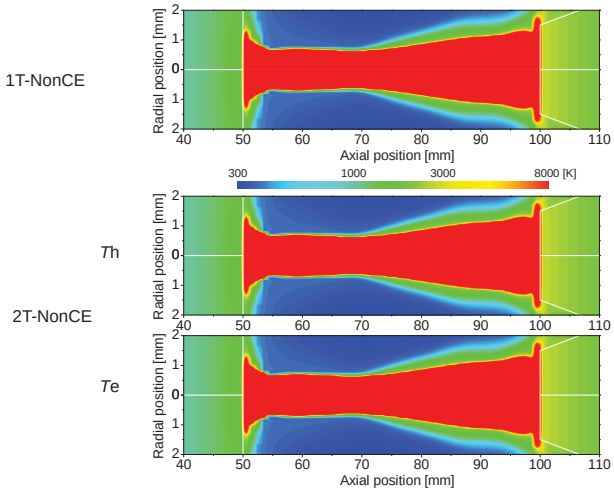

Fig. 3. Temperature distributions between the electrodes in an SF_6 arc at t = 0 μs after current zero. The upper panel is the temperature calculated by the one-temperature chemically non-equilibrium (1T-NonCE) model, the middle and the lower panels are respectively the heavy particle temperature T_h and the electron temperature T_e calculated by the two-temperature chemically non-equilibrium (2T-NonCE) model.

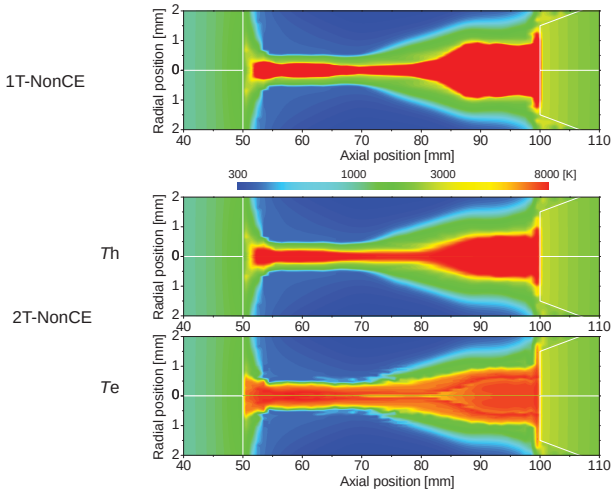

Fig. 4. Temperature distributions between the electrodes in an SF_6 arc at t = 5 μs after current zero. The upper panel is the temperature calculated by the one-temperature chemically non-equilibrium (1T-NonCE) model, the middle and the lower panels are respectively the heavy particle temperature T_h and the electron temperature T_e calculated by the two-temperature chemically non-equilibrium (2T-NonCE) model. TRV is applied with RRRV=0.2 kV/μs.

from the higher thermal conductivity of electrons. Thus, the arc radius defined by T_e is larger than that by T_h. At t = 7 μs after current zero, the instantaneous applied voltage is 0.4 kV. This applied voltage brings a T_e increase in the vicinity of the upstream electrode. At the same time, T_h still decreases with time by convection and thermal conduction losses for heavy particles. At t= 8 μs, T_e in the vicinity of the upstream electrode rises up markedly owing to the joule heating $\sigma_e|E|^2$ there. The T_h here is also heated from the energy conversion from electrons as indicated in Eq.(15). After that, both T_e and T_h are increased rapidly in 1μs, resulting in the interruption failure.

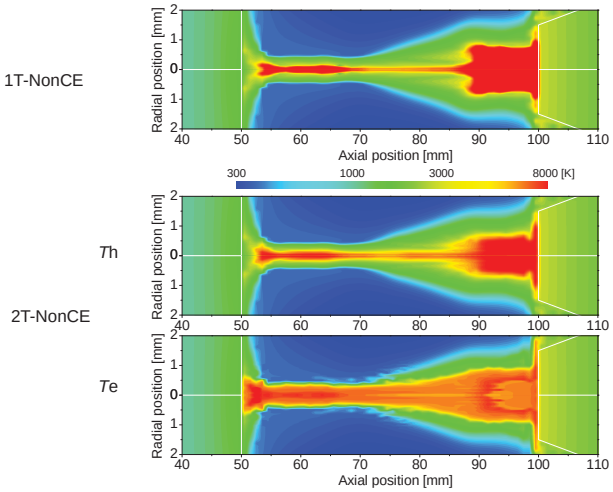

Fig. 5. Temperature distributions between the electrodes in an SF_6 arc at t = 7 μs after current zero. The upper panel is the temperature calculated by the one-temperature chemically non-equilibrium (1T-NonCE) model, the middle and the lower panels are respectively the heavy particle temperature T_h and the electron temperature T_e calculated by the two-temperature chemically non-equilibrium (2T-NonCE) model.TRV is applied with RRRV=0.2 kV/μs.

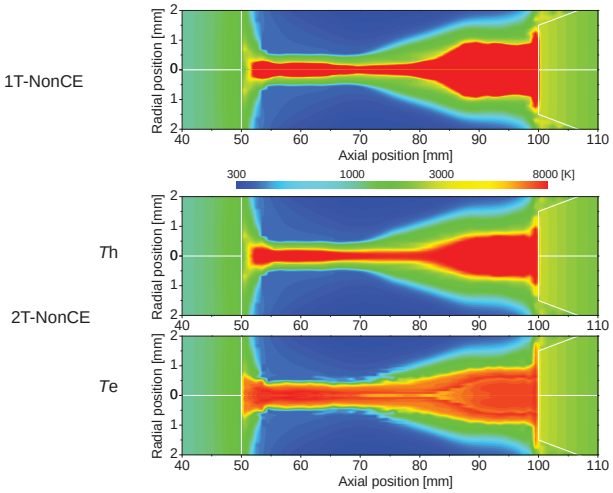

Fig. 6. Temperature distributions between the electrodes in an SF_6 arc at t = 8 μs after current zero. The upper panel is the temperature calculated by the one-temperature chemically non-equilibrium (1T-NonCE) model, the middle and the lower panels are respectively the heavy particle temperature T_h and the electron temperature T_e calculated by the two-temperature chemically non-equilibrium (2T-NonCE) model. TRV is applied with RRRV=0.2 kV/μs.

We compared between results by 2T-NonCE model and 1T-NonCE model. The temperature T by 1T-NonCE model decays from t=0 μs rapidly. The decaying aspect in the T seems similar to that in the T_h. This implies that the energy conservation equation in the 1T-NonCE model expresses almost the heavy particle energy conservation equation in the 2T-NonCE model. This 1T-NonCE model predicted the successful interruption, although the 2T-NonCE model did the interruption failure. This is due to the rapid increase in T_e in the 2T-NonCE model.

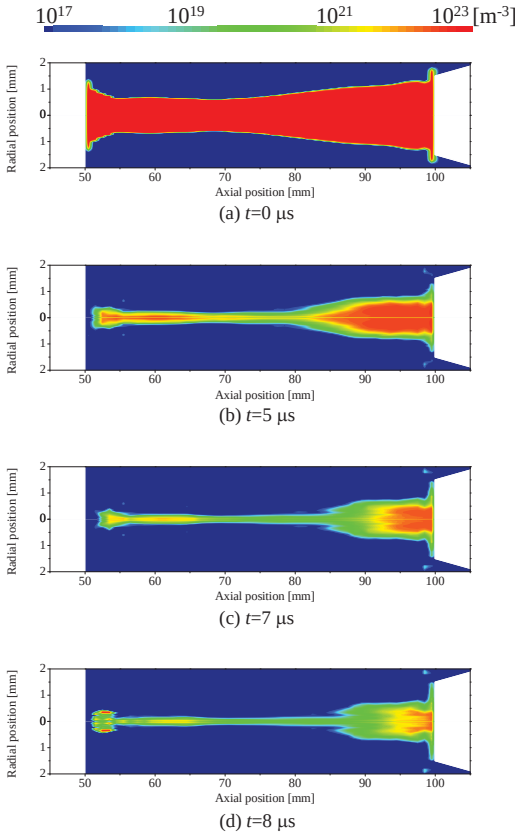

Fig. 7. Electron density distributions between the electrodes in an SF_6 arc after current down calculated by the two-temperature chemically non-equilibrium (2T-NonCE) model. TRV is applied with RRRV=0.2 kV/μs.

IV. Time Evolution in Electron Density

For arc re-ignition process, the recovery of electrical conductivity, and thus the electron density in a residual arc may be essential as well as T_e. Generally, increasing T_e elevates the electron density due to electron impact ionization of heavy particles. Fig. 7 indicates time evolution in electron density in decaying SF_6 arcs with TRV application of a RRRV of 0.2 kV/μs. The electron density decays rapidly, in particular, around the nozzle throat with time from current down. This is due to strong radial convection and radial diffusion effects, as well as dissociative electron attachment reaction $F_2 + e \rightarrow F^- + F$. At t=7 μs, the decay rate in the electron density around an axial position of 60 mm becomes slower on the axis. This is because of electron impact ionization by T_e increase due to joule heating. At t=8 μs, the electron density increases on the axis there and furthermore around the in the vicinity of the upstream electrode. This is one trigger to raise the electron density increase for arc re-ignition. After that, the electron density on the axis between the electrode is elevated promptly. This elevation results in the interruption failure.

V. Summary

In this paper, the two-temperature chemically non-equilibrium model was used to study the effect of transient recovery voltage (TRV) application to residual SF_6

arcs. First, the decaying SF_6 arcs under free recovery condition was created by stepping down the current for a fundamental study. To the decaying SF_6 arcs, the TRV was numerically applied with a rate of rise of recovery voltage of 0.1 kV/μs and 0.2 kV/μs to investigate the arc re-ignition processes. As a result, the application of 0.2 kV/μs TRV causes the arc re-ignition with increasing electron temperature and the electron density near the upstream electrode. It was also found that the temperature evolution by one-temperature model is simulated almost only to the evolution in the heavy particle temperature.

VI. Acknowledgments

The authors would like to thank Mr. T.Iijima and T.Shinkai at Toshiba for their discussions about circuit breaker arcs.

References

[1] Y.Tanaka, Y.Yokomizu, T.Matsubara, T.Matsumura, "Particle composition of two-temperature SF_6 plasma in pressure range from 0.1 to 1 MPa", *Proc. 12th Int. Conf. Gas Discharges & Their Appl.*, vol.II, pp.566–569, 1997.9.

[2] Y.Tanaka, T.Matsubara, Y.Yokomizu, T.Matsumura, T.Sakuta, "Calculation of SF_6 plasma composition in two-temperature steady state using reaction kinetics," *Proc. Int. Conf. on Electr. Eng. ICEE'98*, pp.583–586, 1998.7.

[3] Y.Tanaka and T.Sakuta, "Numerical approach for analysing transient behaviour of SF_6 induction thermal plasma using reaction kinetics", *Proc. 14-th Int. Symp. on Plasma Chem. ISPC-14*, pp.245–250, 1999.8.

[4] R.Girard, J.J.Gonzalez, A.Gleizes, "Modelling of a two-temperature SF_6 arc plasma during extinction", *J.Phys.D:Appl.Phys.*, vol.32, No.11, pp. 1229–1238, 1999.

[5] A.Gleizes, B.Chervy, J.J.Gonzalez, "Calculation of a two-temperature plasma composition: bases and application to SF_6," *J. Phys. D: Appl. Phys.*, vol. 32, No.16, pp.2060–2067, 1999.

[6] R.Girard, J.B.Belhaouari, J.J.Gonzalez, A.Gleizes, "A two-temperature kinetic model of SF6 plasma" *J. Phys. D: Appl. Phys.*, vol. 32, No.22, pp.2890–2901, 1999.

[7] I.Coll, A.M.Casanovas, L.Vial, A.Gleizes, J.Casanovas, "Chemical kinetics modelling of a decaying SF_6 arc plasma in the presence of a solid organic insulator, copper, oxygen and water", *J. Phys. D: Appl. Phys.*, vol. 33, No.3, pp.221–229, 2000.

[8] J.J.Gonzalez, R.Girard, A.Gleizes, "Decay and post-arc phases of a SF_6 arc plasma: a thermal and chemical non-equilibrium model", *J. Phys. D: Appl. Phys.*, vol.33, No.21, pp. 2759–2768, 2000.

[9] Y.Tanaka, K.Suzuki, "Development of a chemically non-equilibrium model on decaying SF6 arc plasmas", *Proc. the First Int. Conf. Electric Power Equip. Switching Technol., ICEPE2011*, pp.492–495, 2011.

[10] Y.Tanaka, T.Shinkai, "Effect of gas flow on decay process in SF6 arcs predicted by a chemically non-equilibrium model", *Int.Conf. Electr. Eng., ICEE2012*, P-PS1-1 , 2012.

[11] Y.Tanaka, T.Shinkai, "Numerical study on particle composition variation in decaying SF6 arc plasmas using a 2D chemically non-equilibrium model" *Proc. 19th Int.Conf. Gas Discharges & their Appl., GD2012*, pp.66–69, 2012.

[12] W.Z.Wang, J.D.Yan, M.Z.Rong, A.B.Murhpy, J.W.Spencer, "Theoretical investigation of the decay of an SF_6 gas-blast arc using a two-temperature hydrodynamic model", *J. Phys. D: Appl. Phys.*, vol.46, 065203, 2013.

[13] Y. Tanaka, Y.Yokomizu, M. Ishikawa and T. Matsumura, "Particle composition of high-pressure SF6 plasma with electron temperature greater than gas temperature", *IEEE Trans. Plasma Sci.*, vol.25, No.5, pp. 991–995, 1997.